

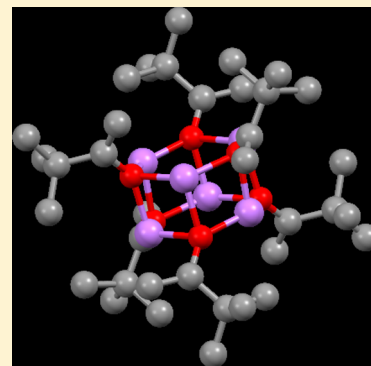
Conformational Polymorphism of Lithium Pinacolone Enolate

Jie Guang, Qiyong Liu,[†] Russell Hopson, Gerald Kagan,[‡] Weibin Li,^{||} Thomas B. Monroe, and Paul G. Williard*

Department of Chemistry, Brown University, Providence, Rhode Island 02912, United States

S Supporting Information

ABSTRACT: A metastable, polymorphic hexameric crystal structure of lithium pinacolone enolate (LiOPin) is reported along with three preparation methods. NMR-based structural characterization implies that the lithium pinacolone hexamer deaggregates to a tetramer in toluene but retains mainly the hexameric structure in nonaromatic hydrocarbon solvents such as cyclohexane. Moreover, the presence of a small amount of lithium aldolate (LiOA) dramatically influences the aggregation state of LiOPin by forming a mixed aggregate with a 3:1 ratio (LiOPin₃·LiOA).



INTRODUCTION

Lithium enolates play an important role in organic synthesis. Furthermore, the mechanism through which they react in solution is complicated and only incompletely understood. Structural information about lithium enolates in solution provides a foundation for detailed mechanistic studies, is challenging to obtain, and is interpreted in comparison with structure–reactivity correlations with other organolithium reagents. Structure–reactivity correlations are available for lithium amide bases and alkyl lithiums for which a wealth of mechanistic information is now available.¹ Therefore, a strategy for correlating enolate solution structure with X-ray crystal structures is important for identifying and for developing a comprehensive understanding of the mechanism and reactivity of lithium enolates.

Solid-state structures provide indirect evidence of the structure of organolithium intermediates in solution. Nonetheless X-ray diffraction (XRD) analysis is the most reliable method to obtain precise and unambiguous structural information, especially for the discovery of lithium enolate complexes that contain ¹H NMR-silent components such as LiOH, LiX, and solvent molecules. Therefore, as a starting point, crystal structures yield crucial models and provide guidelines for interpreting and predicting various possible intermediates in solution.² Since Seebach reported the first two crystal structures of tetra THF-solvated, lithium enolate tetramers in 1981, 29 crystal structures containing lithium, monocarbonyl ketone enolates have been reported. These structures are summarized as follows: three unsolvated hexamers,³ six tetramers (solvated by THF, pyridine, or HMPA),⁴ two solvated (THF or diethyl ether) dimers with bulky substituent groups on the enolate,⁵ three bidentate ligand-solvated dimers,^{3a,6} two tridentate-solvated monomer-

s^{5a,7} and two mixed lithium amide/enolate aggregates,^{4a,8} one mixed lithium hydroxide/enolate aggregate,^{4a} one dimeric dienolate,⁹ four internally chelated enolates,¹⁰ two halide/enolate mixed aggregates,¹¹ and five mixed metal/lithium cation enolate aggregates.¹² cursory review of all these crystal structures strongly suggests to us that the variations of solvation and aggregation states can be rationalized mainly by steric effects. Bulky ligands or large substituent groups on enolates result in lower aggregation degrees or substoichiometric solvation status. However, caution is always necessary when the discussion or assumption of solution-state characterization cites the crystal structures because their status in solution is much more complex and completely unlike single crystals that are relatively pure and not capable of dynamic exchange or equilibria. Hence in solution, all organolithium species that are present not only interact with the solvent/ligand sea around them but also typically exchange with other homo or heteroaggregates coexisting in the solution. It is noteworthy that multidentate N-donor ligands failed to bind and deaggregate the lithium enolate tetramer in THF solution. This is still poorly understood.^{7,13}

In order to characterize the aggregation of lithium enolates in solution, colligative property measurements such as cryoscopy, vapor-phase osmometry, differential pressure barometry, or ebullioscopy, UV–vis spectroscopy, and NMR-based methods have been applied. Colligative methods are not widely used at present due to their sensitivity to impurities, their imprecision, and difficult interpretation when noninteger aggregation states are determined experimentally.¹⁴ The UV–vis spectroscopic method, developed by Streitwieser and co-workers, is powerful

Received: August 5, 2016

Published: October 20, 2016

for measuring equilibrium constants of various lithium enolate intermediates in solution on the basis of changes in UV–vis spectra with concentration, but large aromatic groups are required in the enolate substrates due to the UV spectral requirements.¹⁵ Jackman and co-workers combined colligative measurements, ¹³C spin–lattice relaxation time (T_1) measurement, and ⁷Li quadrupolar splitting constants (QSC) to study the aggregation states of hindered aromatic lithium enolates.¹⁶ Jackman’s protocol requires both the existence of aromatic groups and careful extrapolation from experimental results to the conclusions about aggregation states. More recent NMR-based techniques applied to solution-state characterizations of lithium enolates are roughly divided into three strategies. First, additive titration experiments were used very successfully by Reich and co-workers to map the solvation states of a specific aggregate on the basis of signal ratio and their J-coupling pattern when the additive is HMPA.¹⁷ Second, when direct J-coupling is not an available option, which is typical for lithium enolates because direct ⁶Li–¹⁵N, ⁶Li–³¹P, or ⁶Li–¹³C coupling is not observable, Collum employs a very effective method referred to as continuous variation or “Job plots” to assign the mixed species of two similar lithium enolates.¹⁸ If each mixed aggregate has at least one clear and nonoverlapping signal in their NMR spectrum, then the aggregation states of both lithium enolates can be determined by comparing the ratio of signals of different aggregates with a continuous variation of combinations of the two enolates. Last but not least, our lab has developed and applied a diffusion oriented NMR technique, DOSY, to the analysis of enolate solutions and appropriate internal references to obtain the molecular weight of enolate aggregates by correlating molecular weights with diffusion coefficient values.^{4a} We referred to this technique as diffusion-formula weight (D-FW), or alternatively “referenced diffusion-ordered NMR spectroscopy (rDOSY)”.¹⁹ This method is ideal for determining the aggregation degree of unsolvated lithium aggregates if each lithium species and internal reference has at least one nonoverlapping signal in the NMR spectrum. More recently Stalke and Morris have reexamined this NMR diffusion, molecular-weight correlation.²⁰ For lithium aggregates with binding ligands, we combined titration experiments with crystal structure determinations to determine both solvation states and aggregation states simultaneously using this method.

In this paper, the first structural characterization and the corresponding solution-state aggregation study of unsolvated, conformationally polymorphic lithium enolate is reported.²¹ The crystal structures of a pair of lithium pinacolate hexamer conformational polymorphs are compared and NMR experiments including referenced DOSY experiments are presented. Moreover, in this process, an intriguing mixed aggregate of lithium enolate and lithium aldolate was also discovered and characterized and is discussed. We suggest that this latter structure is likely an important intermediate along the cascade of lithium aggregates that comprise the aldol reaction.

RESULTS AND DISCUSSION

Conformational Polymorphic Crystal Structure of Unsolvated Lithium Pinacolone Enolate Hexamer. *Crystal Preparation.* Three decades ago, we reported a hexameric structure of unsolvated lithium pinacolone enolate (LiOPin) as the first example of an unsolvated lithium enolate.^{3b,22} Several years later, Liu working in the same lab prepared a polymorphic crystal of this enolate via recrystalliza-

tion of this unsolvated hexamer. This new structure was also a hexamer with triclinic unit cell parameters different from the reported structure. In this discussion in order to distinguish between them, we refer to the published hexamer as H_a , and the newer conformational polymorphic hexamer first reported here as H_b . After the first observation of H_b by Liu in approximately 1992, we were unable to obtain H_b again for nearly two decades. This mysterious “disappearing polymorphs” phenomenon is unfortunately not rare in the history of polymorphism study.²³ Only recently we obtained a single crystal of H_b from a pentane solution of LiOPin in the presence of around 0.2 equiv HMPA at $-20\text{ }^\circ\text{C}$. We have now repeated the crystallization of H_b several times using this condition with the presence of $\sim 0.1\text{--}0.2$ equiv HMPA (method 1). Subsequently H_b was also prepared from a toluene solution of LiOPin at $-20\text{ }^\circ\text{C}$ without any additive (method 2). Finally, we also successfully repeated Liu’s procedure of obtaining the H_b crystalline polymorph by recrystallization of H_a in pentane (method 3). Therefore, H_b has been observed repeatedly by X-ray analysis via three different preparation methods. However, it is also noteworthy that the H_a polymorph is also obtained from all of these three preparation methods. This latter observation indicates that a controllable and predictable preparation of H_b is still not available. To date, it is very difficult to predetermine whether any crystallization will yield the H_a or H_b polymorph until X-ray analysis is applied, although the crystal habit frequently provides a visual clue. According to our experimental observations for any of the three preparation methods mentioned above, H_a precipitates within a period of 24 h at $-20\text{ }^\circ\text{C}$ and H_b crystals usually need more than 1 day, 2–3 days are common or sometimes a full week is required, to form at the same temperature, pressure, and concentration. However, we are still not completely confident whether the time required for crystallization is an entirely credible observation that correctly predicts the polymorph that will form.

Structural Characterization. Crystallographic data for both polymorphs are listed in Table 1 for comparison. Both

Table 1. Selected Crystallographic Data of Two Hexameric LiOPin

	H_a	H_b
empirical formula	$C_{36}H_{66}Li_6O_6$	$C_{36}H_{66}Li_6O_6$
crystal system	triclinic	triclinic
space group	$P-1$	$P-1$
cell lengths (Å)	$a = 11.686(8)$ $b = 11.822(7)$ $c = 17.144(17)$	$a = 10.3259(14)$ $b = 10.7672(14)$ $c = 10.8895(15)$
cell angles (deg)	$\alpha = 80.56(7)$ $\beta = 74.08(5)$ $\gamma = 66.35(5)$	$\alpha = 102.936(3)$ $\beta = 115.200(3)$ $\gamma = 99.243(3)$
R factor (%)	7.81	5.51
density ($\text{g}\cdot\text{cm}^{-3}$)	1.02	1.035

crystals exist in the space group $P-1$, in which the only crystallographic symmetry element is an inversion center. By overlaying a plot of the basic hexagonal prismatic cores of both of these structures consisting of only the Li and O atoms (Figure 1), it is apparent that the Li_6O_6 core is not significantly different. However, the major difference between two hexamers is the conformation of two of the pinacolone residues. As shown in Figure 2, all six *tert*-Bu groups are oriented toward the top and bottom hexagonal faces of the Li_6O_6 core in H_a . Hence,

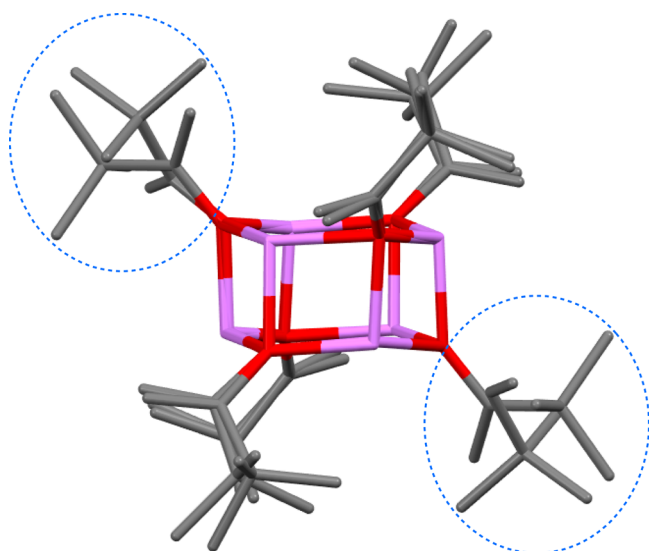


Figure 1. H_a/H_b overlay: Structural differences between two LiOPin hexamers. Hydrogen atoms have been omitted for clarity.

each of the six carbon–carbon, enolate double bonds uniquely approach one of the six side faces of the hexagonal prism. This conformation permits a significant interaction between the electron density in the π -bonds of each enolate residue with a single unique Li^+ cation in this hexamer. However, the major difference observed in structure of H_b is a bond rotation of approximately 120° around the enolate C–O bond in only two enolate residues such that only four of the enolate, carbon–carbon double bonds are located on the side faces of the hexagonal prism. This conformation does not permit the electron density in the oxallyl- π system of two enolates in this polymorph to interact with a Li^+ cation. Consequently, two *tert*-Bu groups from these differently oriented pinacolate residues are located on two of the side faces of the hexagonal prism. The most significant consequence of this structural change is the loss of two Li-oxallyl cation- π interactions. In the H_a

polymorph, each terminal enolate methylene carbon is nearly 0.7 Å closer to one specific lithium atom out of the total of three lithium atoms directly associated with the enolate oxygen of the enolate residue. This observation strongly implies the existence of a single cation- π interaction between lithium and oxallyl groups of each enolate. In each hexameric unit of H_a , there are six pairs of such Li-oxallyl interactions. These interactions are characterized by a close contact of between 2.42 and 2.58 Å between the terminal methylene carbon in the enolate and a lithium cation, as depicted in the left part of Figure 2. However, there are only four pairs of these close cation- π interactions in each hexamer of H_b , as shown in the right part of Figure 2. Due to the rotation of two oxallyl groups, two carbon–carbon double bonds point completely away from lithium atoms preventing any close cation- π interactions for these two enolates. Thus, distances between lithium and terminal methylene carbon are enlarged to an average of 3.72 Å, which is significantly larger than the close ~ 2.5 Å distance observed when the cation- π interaction exists. We also note that the conformation of all six enolate residues in the hexameric, hexa-THF solvated potassium enolate of pinacolone adopts this rotated conformation.²² From Table 1 we also note that the density of the H_b polymorph is larger than the H_a polymorph, reflecting the small increase in volume required to accommodate the conformational change.

Another structural consequence of conformational rotation is the potential steric effect between *tert*-Bu groups. In Figure 3, the viewer observes the two structures from the top of the hexagonal prism, i.e., by directly viewing a hexagonal face of the aggregate. Six *tert*-Bu groups are oriented clockwise in H_a which incorporates a noncrystallographic six-fold rotation/reflection symmetry axis through the centers of the hexagonal faces. Each *tert*-Bu group in this structure is separated from the adjacent one by a carbon–carbon double bond. However, this rotation/reflection symmetry does not exist in H_b . In the structure of H_b , Figure 3 right, the potential steric effect due to two head-to-head *tert*-Bu groups is circled by a blue dashed line, and the 6-fold rotation/reflection symmetry is reduced to 2-fold rotation symmetry.

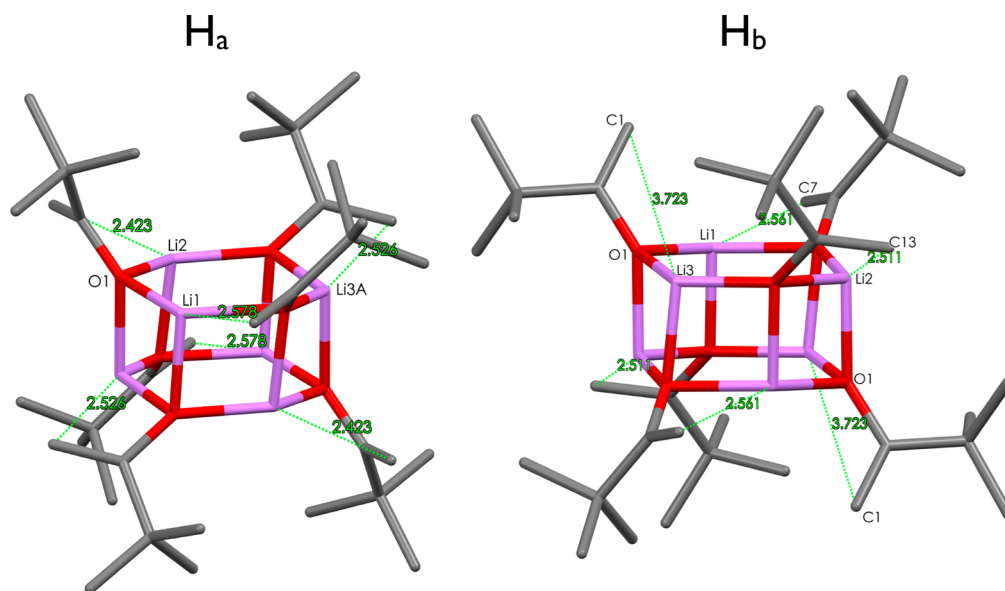


Figure 2. Short distances between lithium atoms and terminal methylene carbons indicate the existence of cation- π interactions. Distances are marked in green values with the unit shown as Å.

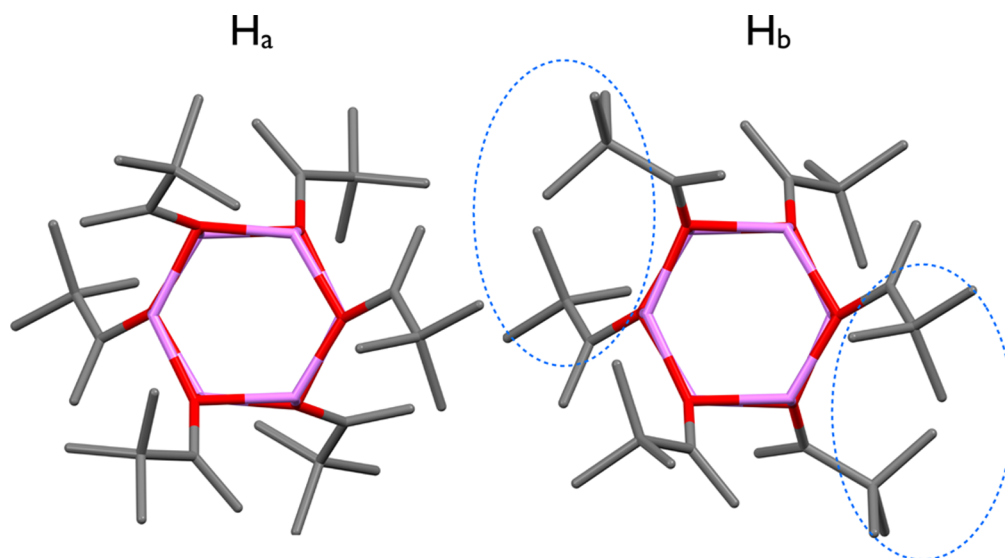
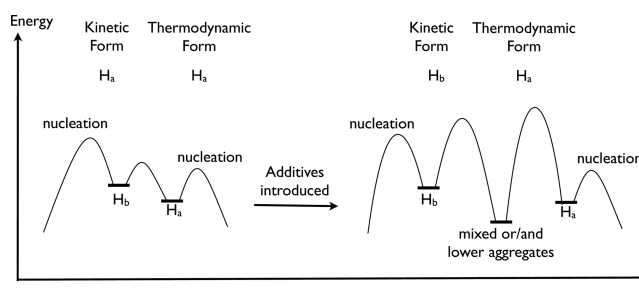


Figure 3. Hexameric structure of H_a and H_b , observed from top. Hydrogen atoms have been omitted for clarity.

Considering the existence of both cation– π interactions and steric effects between *tert*-Bu groups, we suggest that H_b is a metastable conformational isomer slightly less stable than H_a . Considering the experimental observations noted above that the formation of crystal H_a requires a shorter time than the formation of crystal H_b , we suggest that H_a is the thermodynamic form and that it exhibits kinetic crystallization. Therefore, H_a crystallizes first from the mother liquor. Perhaps crystallization of H_b is a consequence of Ostwald's rule.²⁴ All the conformers are likely to coexist in the solution, and usually the most stable form can be crystallized by suppressing the nucleation of other kinetic crystallization forms since the process of crystallization is primarily kinetic.²⁵ Hence, if H_b becomes kinetically favored to crystallize by changing the conditions of crystallization to suppress the nucleation of H_a , then the chance of observing H_b will significantly increase. This change in experimental conditions for kinetic crystallization usually involves temperature,²⁶ pressure, concentration, solvent, and/or additives. All three methods we mentioned previously keep the first three factors fixed. Our three methods for obtaining H_b involve either changing solvent or introducing additives. An aspect common to our three methods for obtaining H_b involves the presence of intermediates in solution which are significantly different from either H_a or H_b . Based on our previous study of HMPA solvated LiOPin, we have demonstrated that adding a small amount of HMPA can effectively influence the aggregation state of LiOPin from hexamer to monosolvated tetramer or even to mixed aggregates that cocrystallize with LDA.^{4a} In this paper, we note that using toluene as solvent to replace pentane leads to the deaggregation of LiOPin hexamer. Moreover, we also report that our recrystallization of H_a crystals introduces lithium aldolate into the solution which also induces the formation of a lower or mixed aggregate (*vide infra*). Therefore, as shown in Scheme 1, we propose that the optimized strategy for obtaining H_b invokes the presence of stable, novel aggregates coexisting in the solution with H_a and H_b and furthermore that their presence favors the kinetic crystallization of the H_b conformational polymorph.

Solution-State Structure of Unsolvated Lithium Pinacolone Enolate. Discrimination of H_a and H_b by

Scheme 1. Proposed Mechanism for the Conformational Polymorphism of Lithium Pinacolone Enolate Hexamer



NMR. Dissolving either a crystal of H_a or H_b in toluene- d_6 yields identical, one-dimensional NMR (^1H , ^{13}C , ^6Li) spectra. However, three different terminal methylene ($=\text{CH}_2$) carbons are observed in the ^{13}C NMR (Figure 4) at -20°C . These correlate with three pairs of terminal methylene proton peaks in the ^1H NMR (Figure 5), as confirmed by $\{^1\text{H}, ^{13}\text{C}\}$ HSQC (Figure S2). These $=\text{CH}_2$ proton peaks are correlated to two lithium peaks in the ^6Li NMR spectra (Figure S4), as confirmed by a $\{^1\text{H}, ^6\text{Li}\}$ HMBC experiment (Figure S5). These NMR results all suggest that at least three LiOPins coexist in the solution and bear different chemical environments. We name these as E, E', and E''. E and E' are the two major components, and E'' is a minor component. The ratio of E to E' dramatically varies among different samples. But the amount of E'' is always less than E'. Above 0°C , peaks belonging to E'' overlap with E' in both ^1H and ^{13}C NMR spectra.

Our first assignment of E and E' is that they are two different hexamers in solution. We propose that E corresponds to H_a and that E' is H_b . It also appeared that E'' is an aggregate with unknown stoichiometry. Moreover, we assume E and E' are in equilibrium in the solution. This explains why the NMR spectra of samples prepared from the pure crystalline H_a and H_b are identical. However, these assignments are not completely consistent with two additional experimental facts. First, by integration, the ratio of terminal methylene protons between E and E' undergoes no observable change in a variable-temperature (VT) NMR experiment from -20°C to -70°C . Second, the self-diffusion coefficient values of E and E', as

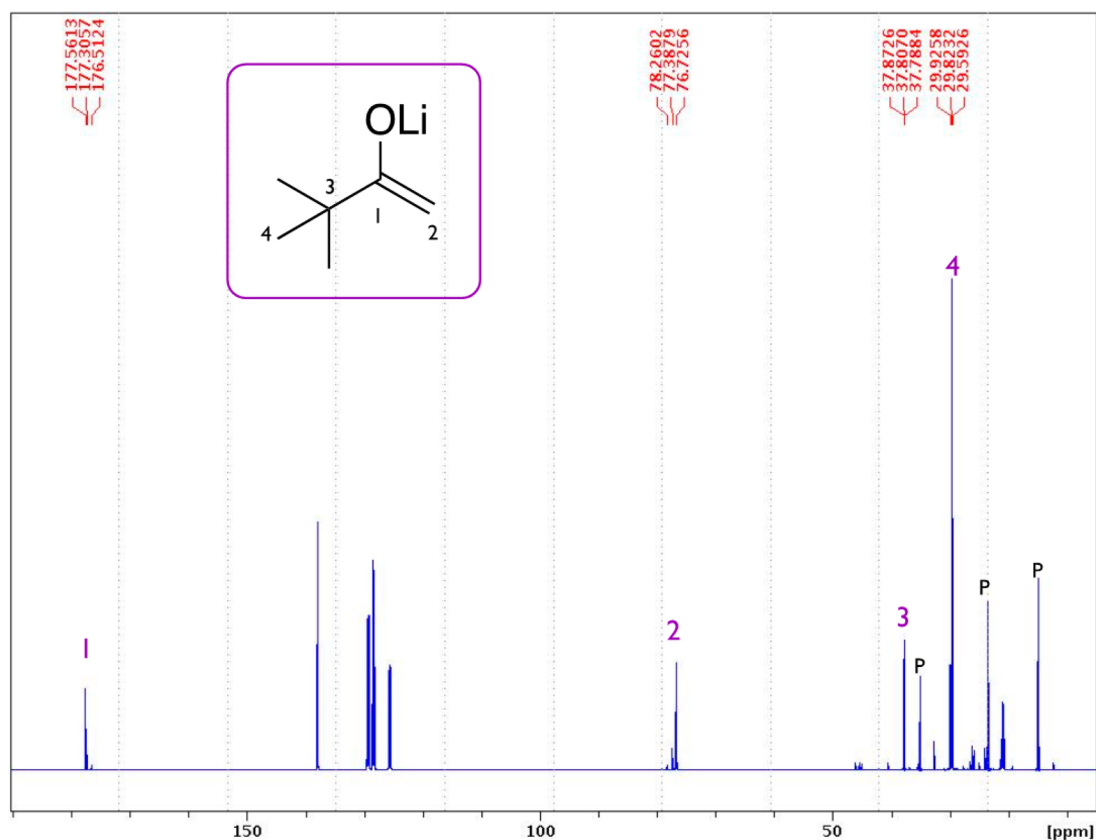


Figure 4. ^{13}C NMR of LiOPin hexamer crystal dissolved in toluene- d_8 at $-20\text{ }^\circ\text{C}$. Three sets of LiOPin peaks are labeled with their chemical shift values. P presents pentane.

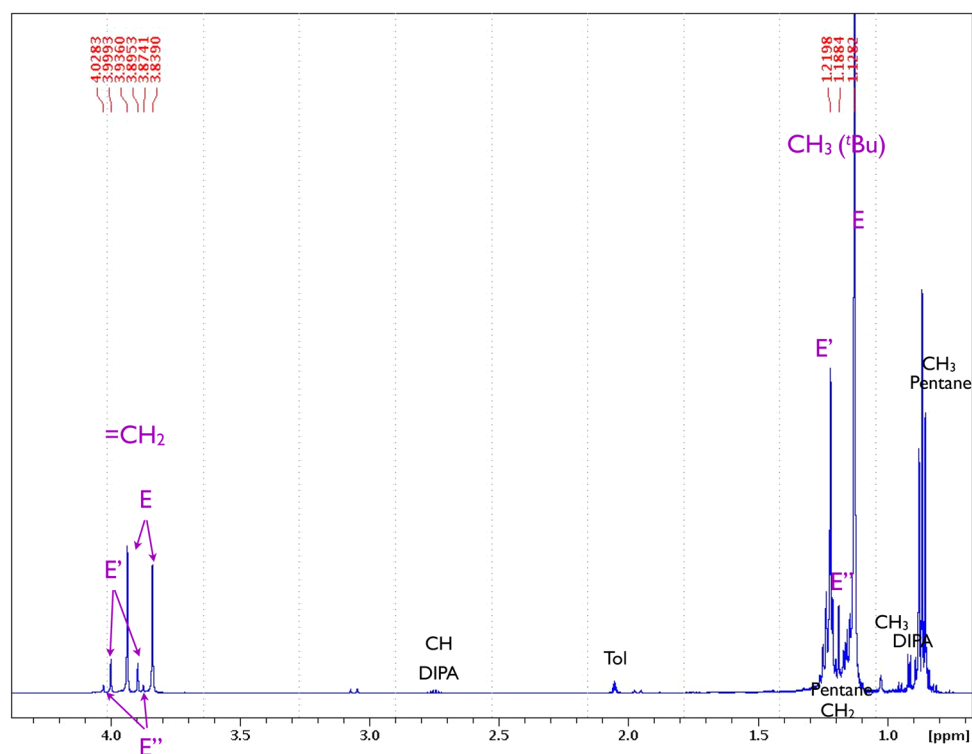


Figure 5. ^1H NMR of LiOPin hexamer crystal dissolved in toluene- d_8 at $-20\text{ }^\circ\text{C}$. Three sets of LiOPin peaks are labeled with their chemical shift values. Solvent pentane and a little of diisopropylamine (DIPA) are also observed as impurities.

measured via diffusion oriented NMR (DOSY), always indicate that E' is slightly larger than E. The first fact rejects the

existence of an NMR observable equilibrium between E and E'. The second observation conflicts with the hypothesis that E

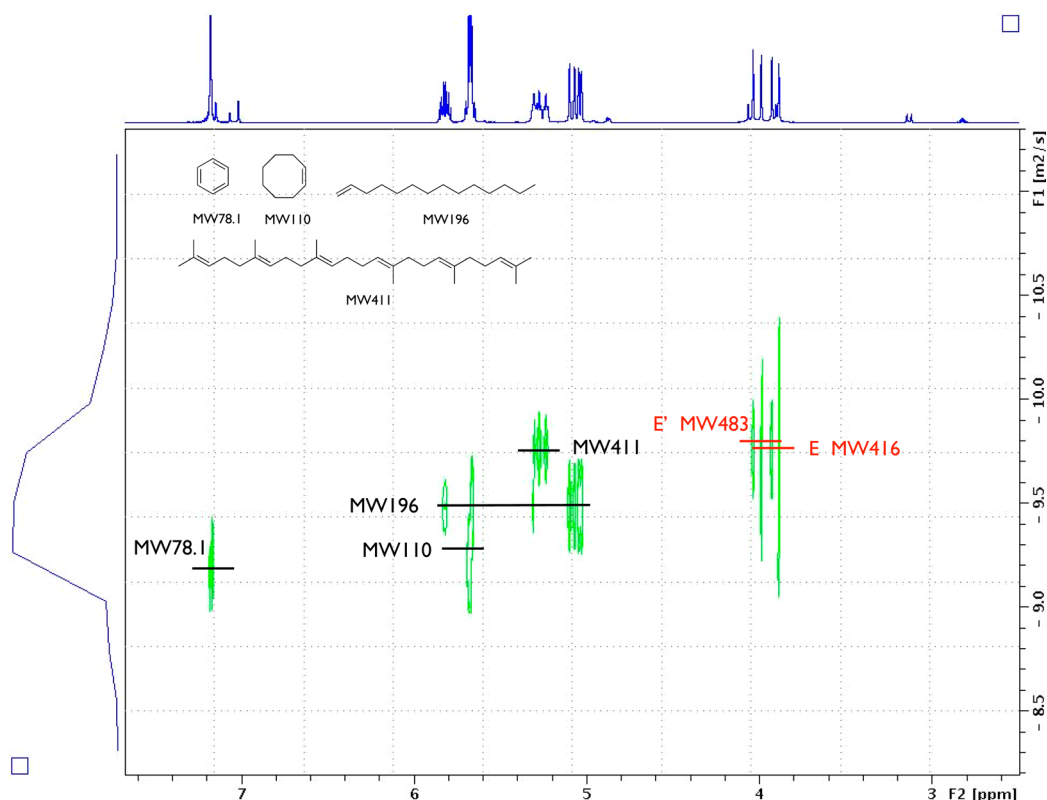


Figure 6. ^1H DOSY spectra of LiOPin hexamer crystal dissolved in toluene- d_8 at $-20\text{ }^\circ\text{C}$.

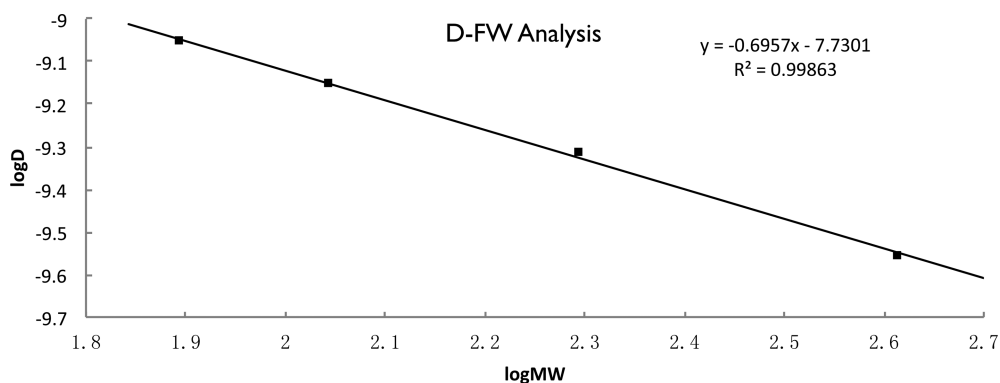


Figure 7. D-FW analysis of ^1H DOSY data of LiOPin hexamer crystal dissolved in toluene- d_8 at $-20\text{ }^\circ\text{C}$.

and E' are both LiOPin hexamers, although a difference in hydrodynamic radii between two hexamers may account for the difference in their observed diffusion coefficient by NMR.

Spectra Interpretation. An alternative proposal that we favor is that the two major components in solution are lithium pinacolate tetramer and hexamer. Considering that by the diffusion NMR results the molecular size of E is smaller than E', E could be assigned as a tetramer, and E' is a hexamer. In order to test this assignment, a referenced DOSY experiment was introduced to measure the molecular weights (MWs) of E and E' in toluene at $-20\text{ }^\circ\text{C}$. As shown in Figures 6 and 7, the diffusion coefficient values of four internal references in solution with E and E' were measured, and MWs of E and E' were determined based on D-FW analysis (Table 2). The MW expected for an unsolvated LiOPin tetramer is 424 g/mol and for an unsolvated hexamer is 636 g/mol. The experimentally observed MW of E is 416 g/mol, which is quite close to the value of tetramer with a -2% error. However,

Table 2. D-FW Analysis of ^1H DOSY Data of LiOPin Hexamer Crystal Dissolved in Toluene- d_8 at $-20\text{ }^\circ\text{C}$

entry	compd	FW (g/mol)	D (m^2/s)	predicted FW (g/mol)	% error
1	BEN	78.1	8.895×10^{-10}	79.2	1
2	COD	110	7.041×10^{-10}	111	1
3	TDE	196	4.858×10^{-10}	189	-4
4	SQU	411	2.789×10^{-10}	419	2
5	E	424	2.802×10^{-10}	416	-2
6	E'	—	2.528×10^{-10}	483	—

if E' is a hexamer, then the experimental error is -24% . Based on all of our previous experience with referenced DOSY experiments, an experimental absolute error of $<10\%$ from a calculated MW is routine, and typically this error is $<6\%$. Thus, this D-FW result is also not fully consistent with the fact that E' is assigned as an unsolvated hexamer. Even though the

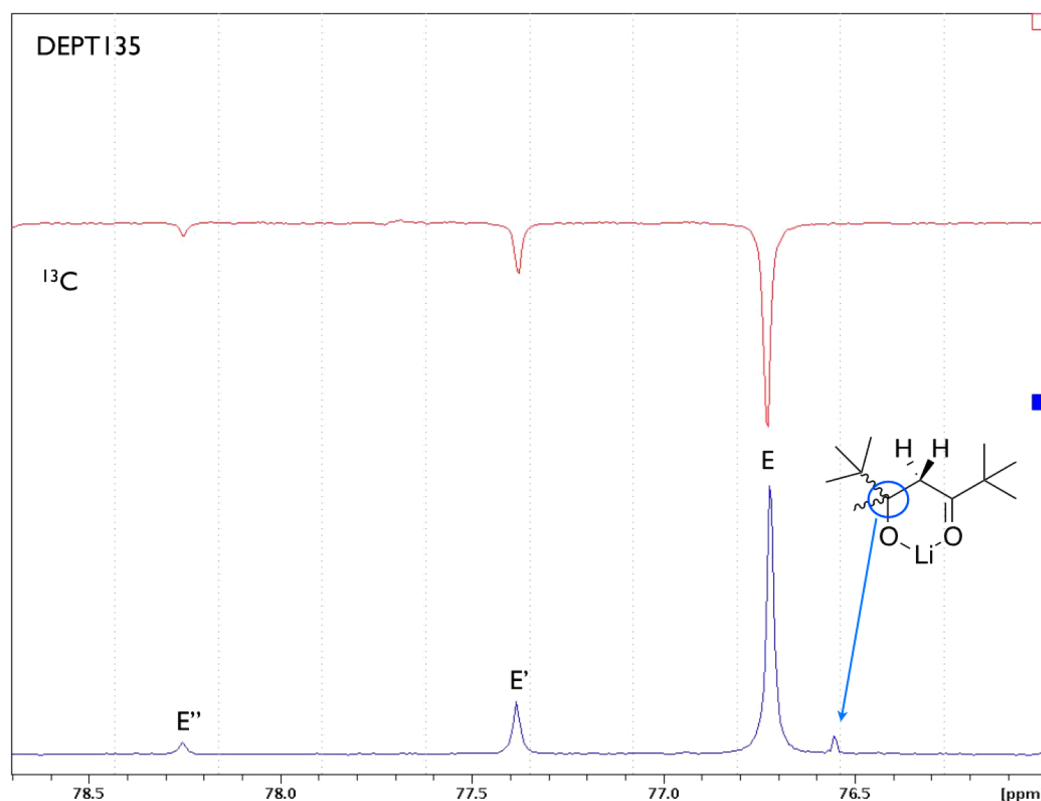


Figure 8. Overlay of ^{13}C NMR and DEPT-135 spectra. Three terminal methylene carbons from three different enolates show a negative phase in DEPT-135, and a quaternary carbon from aldolate would only be present in ^{13}C NMR but not DEPT-135 spectra.

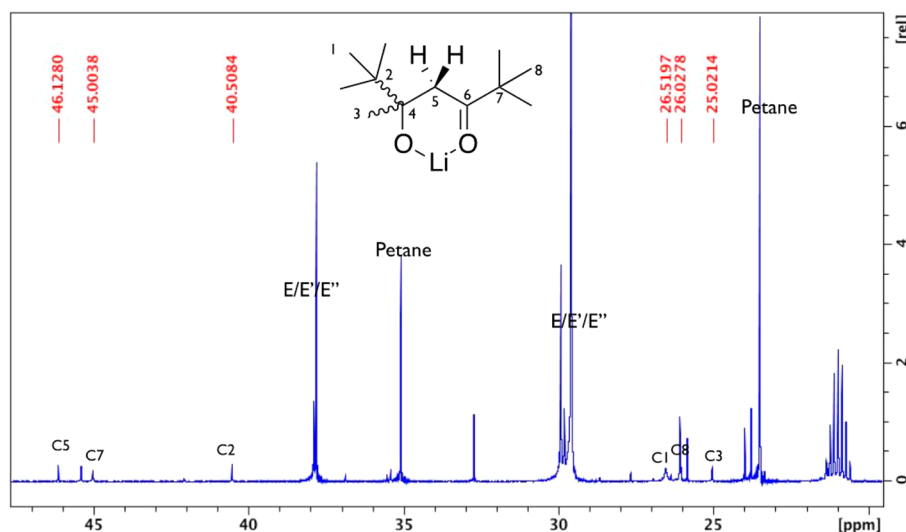


Figure 9. Upfield region (10–50 ppm) of ^{13}C NMR of LiOPin hexamer crystal dissolving in toluene- d_3 at $-20\text{ }^\circ\text{C}$.

experimentally observed MW of E' (483 g/mol) approaches the MW of LiOPin pentamer (530 g/mol) with a 9% error, we are hesitant to assign E' as a pentamer, because pentameric organolithium aggregates have never been observed in solid state and are also very rare in solution state.²⁷

We applied the referenced DOSY experiment to another sample with a different ratio of E to E' at $-50\text{ }^\circ\text{C}$, a conspicuously lower temperature than $-20\text{ }^\circ\text{C}$. Quite similar results were obtained with the experimentally observed MW of E as 430 g/mol and E' as 491 g/mol (Figures S11 and S12 and Table S2). These repeatable temperature-independent MW

values enhance the reliability of the referenced DOSY experimental observations and also likely rule out the possibility that the NMR peak we monitor and assign to E' corresponds to overlapping, unresolved peaks from the exchange between a tetramer and a hexamer.

After careful review of all the spectra, we noted an interesting quaternary carbon peak in addition to the three $=\text{CH}_2$ carbons by overlaying ^{13}C spectra with DEPT-135 spectra (Figure 8). A quaternary carbon peak appearing at 76.5 ppm implies that it is adjacent to electron-withdrawing atoms or groups, which is quite possible for a lithium aldolate, the self-aldol product from

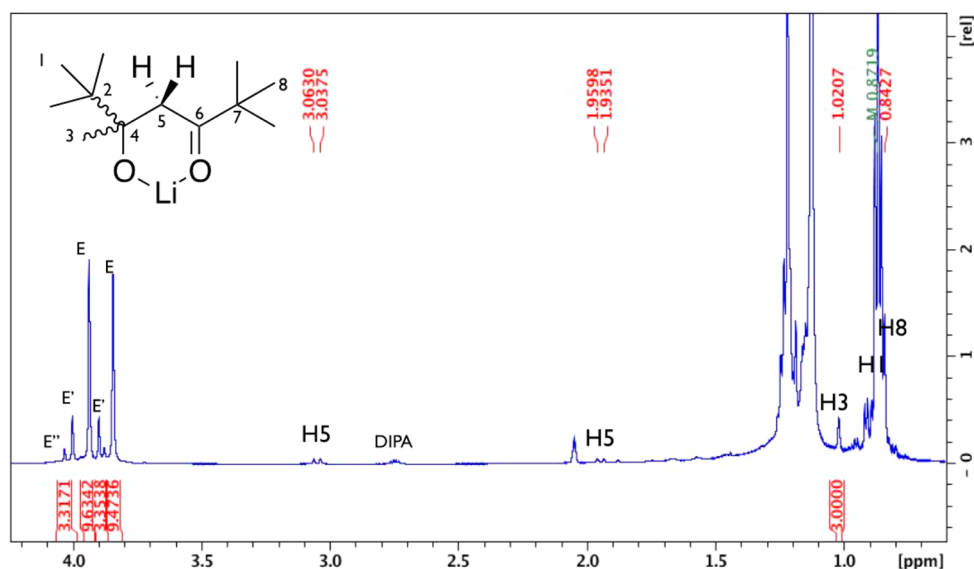


Figure 10. ^1H NMR of LiOPin hexamer crystal dissolving in toluene- d_8 at -20 $^\circ\text{C}$.

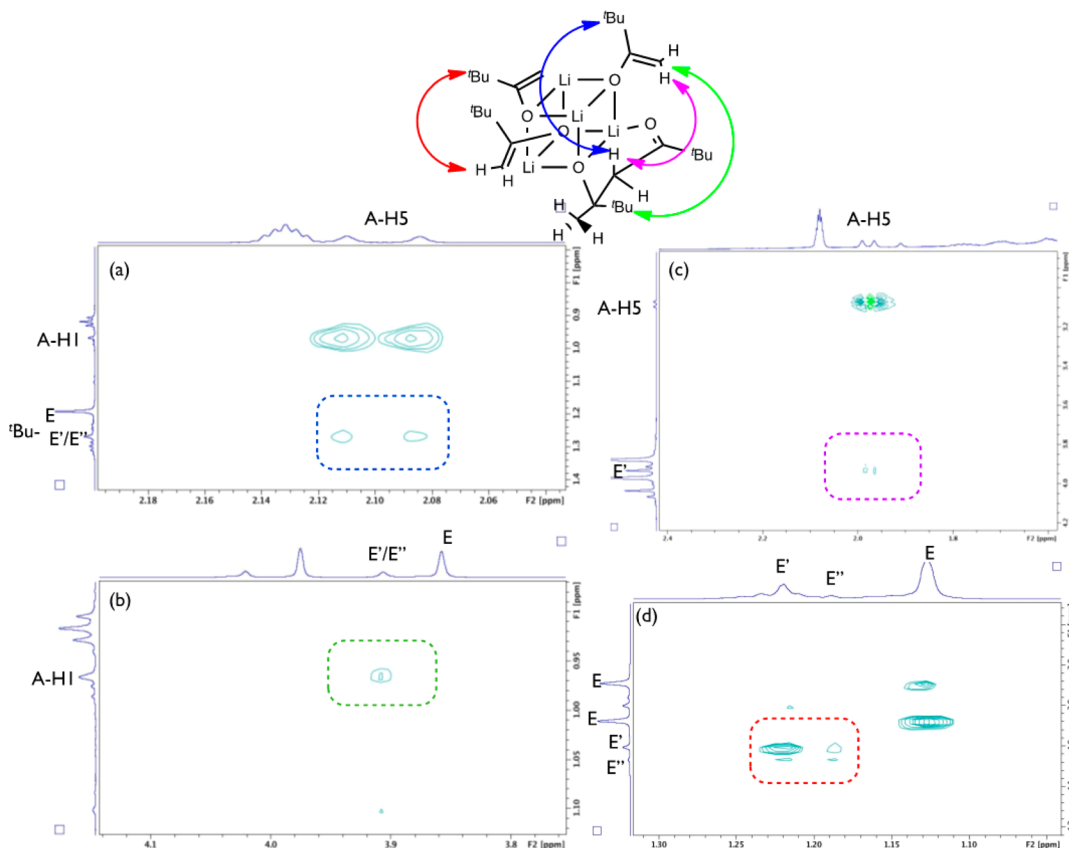


Figure 11. $\{^1\text{H}, ^1\text{H}\}$ NOESY spectra of LiOPin and LiOA in toluene- d_8 : (a) and (b) at 20 $^\circ\text{C}$; (c) and (d) at -30 $^\circ\text{C}$.

LiOPin and pinacolone. Aldolate is a reasonable byproduct or impurity in this system, because during the storage, wash, and transfer of the crystalline samples, a small amount of LiOPin can be quenched to form pinacolone followed by self-aldol reaction proceeding very fast at room temperature. We had not considered the possible presence of aldolate until noticing this quaternary carbon. Since only three downfield oxygen bearing carbons are depicted in the ^{13}C spectra at 177.6, 177.3, and 176.5 ppm (Figure 4), and these are correlated with three

terminal methylene carbons, they all must belong to lithium enolates. However, the existence of lithium aldolate requires a carbonyl peak in the ^{13}C spectra. After expansion of the spectral width (sw) to 260 ppm, we did observe the expected aldolate carbonyl carbon peak at 224.4 ppm (Figure S6). This downfield chemical shift value supports the structure drawn below with a lithium cation solvated by a carbonyl oxygen in an aldolate residue. Furthermore, the downfield shift of this carbonyl peak is attributable to diminished electron density due to

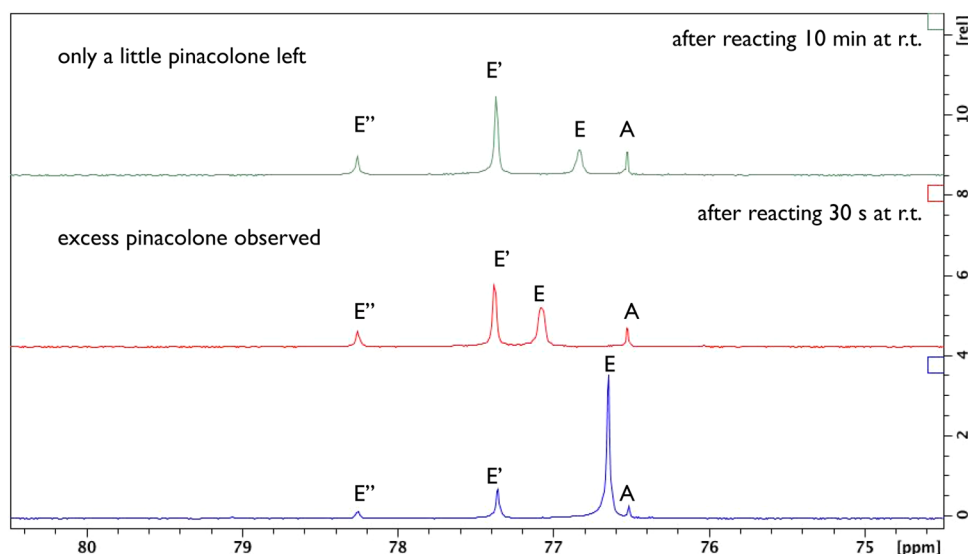


Figure 12. Overlay of ^{13}C NMR spectra of adding pinacolone to the solution of LiOPin hexamer crystal in toluene- d_8 at $-30\text{ }^\circ\text{C}$. E', E'', and A increase comparing with E. A presents lithium aldolate.

coordination to the Li^+ cation in the aldolate. All other carbon and proton peaks belonging to lithium aldolate were subsequently observed and assignable in both ^{13}C and ^1H spectra (Figures 9, 10, and S6) with the help of HSQC, HMBC, and NOESY spectra (Figures S1–S3).

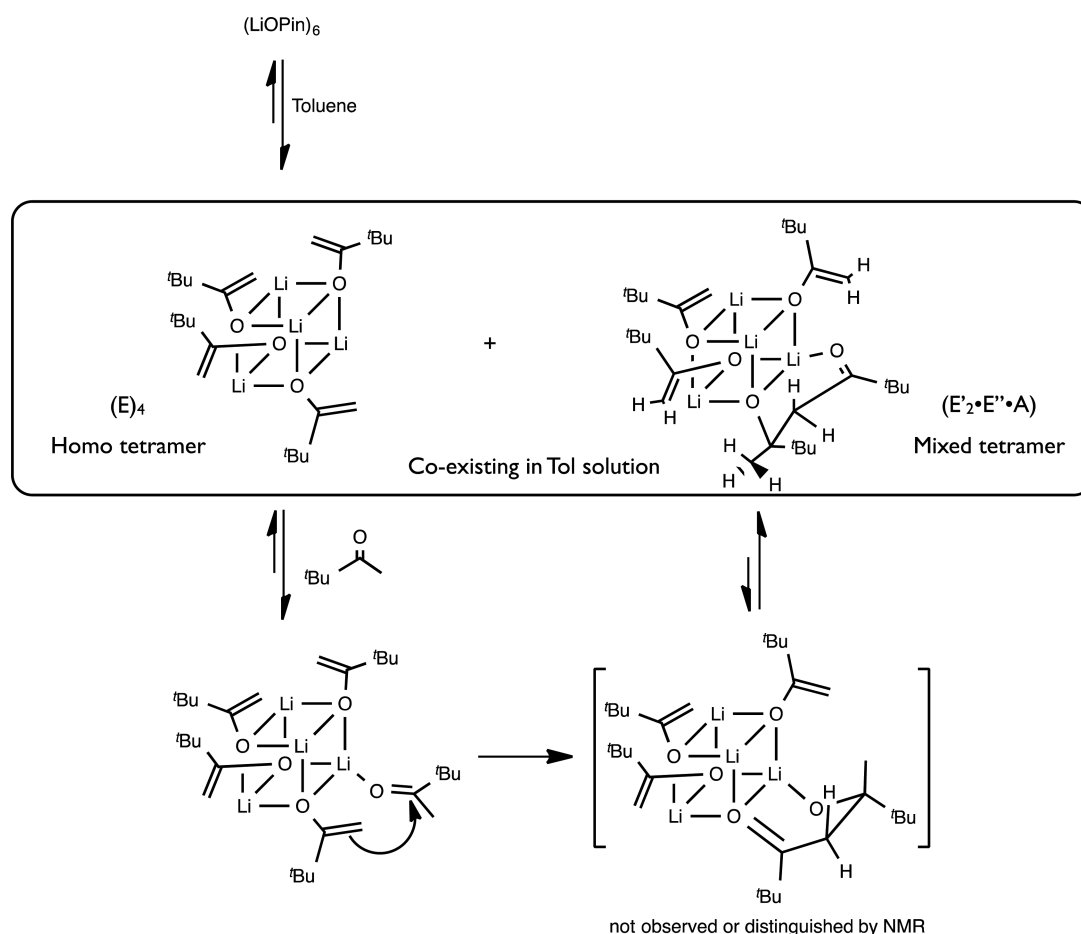
Since all the NMR data now support the existence and the presence of some lithium aldolate in these samples, we deduced that the NMR peaks we assign to E' belong to a mixed aggregate of LiOPin and lithium pinacolone aldolate (LiOA). This assumption is confirmed by NOE experiments (Figure 11). Hence, the methylene proton H5 (Figures 9 and 10) of aldolate presents an NOE with both methylene proton (Figure 11c) and *tert*-butyl proton (Figure 11a) forms of enolate E'. Also, the methyl proton H1 in the aldolate exhibits a NOE with one of the two methylene protons from E' (Figure 11b). This means E' binds with lithium aldolate and forms a mixed aggregate. Moreover, as shown in Figure 11d, there are NOE cross peaks between the methylene protons and *tert*-butyl protons of E' and E''. Therefore, the mixed aggregate contains not only E' and aldolate but also E''. This conclusion is also supported by the fact that peaks belonging to E', E'', and aldolate will increase, and the ones from E will decrease if a small amount of pinacolone is added to the solution (Figures 12, S7, and S8). Following up on this latter observation, we also noticed that upon adding trace quantities of free pinacolone to these enolate crystal solutions, the signals for the species assigned as E experience a significant change in chemical shift in all ^1H , ^6Li , and ^{13}C NMR spectra. Meanwhile, peaks belonging to the mixed aggregate do not undergo any obvious shifts. These observations imply that any excess unenolized, pinacolone binds to homo tetramer in preference to binding with the coexisting mixed aggregates in toluene solution.²⁸ It is also noteworthy that the tetrameric sodium enolate of pinacolone solvated by pinacolone has been characterized.²²

Considering that the experimentally observed MW of E' is 483 g/mol from the referenced DOSY experiment, we conclude that this mixed aggregate is a tetramer consisting of LiOPin and LiOA with ratio of 3:1 (calculated MW is 524 g/mol). To the best of our knowledge, a crystal structure of mixed aggregate consisting only of lithium enolate and lithium aldolate has not

been observed to date. However, there are already two crystal structures of unsolvated lithium aldolate that have been reported, both of which are tetramers.²⁹ Hence our observation of a 3:1 stoichiometric mixed aggregate consisting of three parts lithium enolate and one part aldolate is intriguing and not completely understood.³⁰ Furthermore, Reich and co-workers have reported comprehensive work on the aldol reaction between 4-fluoroacetophenone and 4-fluorobenzaldehyde utilizing LDA.³¹ According to their ^{19}F NMR results, they only observed two mixed aggregates of enolate and aldolate during the aldol reaction in ethereal solvent: a dimer with a stoichiometric 1:1 ratio derived from metastable homoenolate dimer and a 3:1 enolate-aldolate tetramer coming from stable homoenolate tetramer. No 2:2 or 1:3 ratio enolate-aldolate mixed aggregates were observed during the process of aldol reaction in Reich's study. It seems most likely that the same 3:1 enolate-aldolate mixed aggregate observed by Reich using 4-fluoro aromatics is the same as we have observed with pinacolone.

Another question is why the LiOPin hexamer crystal dissolved in toluene deaggregates to a tetramer? In the solid state, lithium cations are stabilized by oxallyl groups as noted above. We suggest that when a LiOPin hexamer is surrounded by a large amount of toluene, the toluene can compete with the oxallyl group for solvating the lithium cations via a lithium- π interaction.³² Therefore, toluene can more easily deaggregate a hexamer to a tetramer. Even though there are no enolate crystal structures containing benzene or toluene as donating ligands to lithium atoms, lithium is known to sit in the center of an aromatic ring, as has been observed in the solid state with many other substrates. Moreover, when we dissolve any LiOPin hexamer crystal in cyclohexane- d_{12} , the species E is observed and exhibits a much larger MW value (548 g/mol) than expected even at room temperature (Figures S9 and S10 and Table S1). These observations clearly suggest to us that we are observing a secondary shell interaction in the diffusion experiments and that toluene can stabilize the tetrameric aggregate perhaps via a cation- π interaction.³³ This explanation is reminiscent of Collum's solution-state study of lithium bis(trimethylsilyl)amide (LiHMDS) in which he utilized ^6Li -

Scheme 2. LiOPin Hexamer Deaggregates to a Tetramer in Toluene and Forms a Mixed Aggregate with LiOA



detected ¹⁵N zero-quantum NMR spectra techniques on [⁶Li, ¹⁵N]LiHMDS.³⁴ Collum also confirmed the existence of a cyclic dimer in toluene and a mixture of oligomers in pentane.

Three intriguing observations from our unsuccessful attempts to crystallize a 3:1 ratio lithium enolate-aldolate mixed aggregate are noted as follows. First, by cooling a hydrocarbon solution of an initial 4:1 stoichiometric ratio of lithium enolate-aldolate mixture, LiOPin hexamer crystals were collected. Both **H_a** and **H_b** have been observed by XRD analysis. This represents yet a fourth method for obtaining the conformational polymorph **H_b**, albeit not very practical. However, as discussed previously (Scheme 1), we believe that the key for forming **H_b** is the existence in solution of mixed or lower aggregates. Therefore, we believe this fourth procedure of obtaining **H_b** probably has the same effect as recrystallization of **H_a** (method 3), wherein a mixed enolate-aldolate aggregate existed in the mother liquor.

Second, a 3:1 ratio of lithium enolate-aldolate mixture solution in pentane or toluene will not give any precipitate even at $-80\text{ }^{\circ}\text{C}$ for 1 week. It seems likely that the 3:1 lithium enolate-aldolate mixed aggregate is very soluble in these solvents. However, after storing at $-20\text{ }^{\circ}\text{C}$ for weeks or even more than one month, a colorless crystal was obtained and analyzed. This crystal is the lithium mixed anion aggregate containing one lithium aldolate, three lithium aldolate dianions, and one unreacted pinacolone molecule, i.e., {^tBuCOCH₂C(=O)MeOLi·3^tBuC(OLi)=CHC(=O)MeOLi·^tBuCOMe}, that has been previously reported by our group utilizing an alternative crystallization procedure.³⁵ For the present purpose,

we thoroughly analyzed a sample of this pure crystalline material, and we now report the NMR spectra of this crystal dissolved in toluene-*d*₈ (Figures S13–15). These new NMR spectra confirm that this unusual LiOA aggregate is observable by NMR but is not present in any significant amount. Moreover, lithium aldolate dianions have never been previously detected in the mixture of lithium enolate and aldolate by NMR, possibly because the basicity of enolate is not strong enough to enolize the lithium aldolate. Hence we now suggest that the driving force for maximizing formation of this unusual lithium mixed anion aggregate that contains lithium pinacolone dianion is its crystallization.

Finally, we observe that upon storing a 3:2 ratio of lithium enolate-aldolate pentane solution at $-20\text{ }^{\circ}\text{C}$ overnight, colorless crystals precipitate. NMR analysis of these crystals in toluene-*d*₈ reveals that the only lithiated component in this NMR sample is the homolithium aldolate aggregate and neither enolate nor enolized aldolate was detected (Figure S16–21). At least nine different LiOAs are distinguishable in these NMR spectra. We interpret this to strongly suggest that LiOA aggregates form diastereomers. Until now, the two reported lithium aldolate crystal structures are both tetramers, and they do not contain a chiral center. Thus, a stoichiometric 3:1 enolate-aldolate mixed aggregate is at least as favorable as the 1:1 or 2:2 enolate-aldolate aggregates in our pinacolone-toluene system. We conclude that the 3:1 enolate-aldolate mixed aggregate is highly soluble and is indeed the dominant mixed aggregate in the hydrocarbon solution of lithium pinacolone and its lithium aldolate.

CONCLUSION

A conformational polymorphic crystal of LiOPin hexamer was prepared via three methods. It is a metastable structure due to the absence of Li-oxallyl cation- π interactions. An NMR study suggests that LiOPin hexamer will deaggregate to mainly tetramer in toluene solution but will remain mainly as a hexamer in cyclohexane solution, as depicted in Scheme 2. We invoke a cation- π interaction between lithium and toluene to explain this behavior. A small amount of lithium aldolate was observed, and this forms a mixed tetrameric aggregate with lithium enolate in a 3:1 enolate/aldolate ratio. This mixed aggregate is the dominant mixed aggregate in the mixture of LiOPin and aldolate. Since it contains only one stereogenic carbon center, it is not prone to form a complicated mixture of diastereomeric aggregates due to the absence of two or more carbon stereogenic centers.

EXPERIMENTAL SECTION

Procedures for NMR Experiments. NMR samples were prepared in tubes sealed with a rubber septa cap and parafilm. NMR tubes were evacuated *in vacuo*, flame-dried, and filled with argon before use. ^1H chemical shifts were referenced to toluene- d_8 at 7.00 ppm, and ^{13}C chemical shifts were referenced to toluene- d_8 at 137.86 ppm. All NMR experiments were acquired on a 600 MHz spectrometer equipped with a z -axis gradient broad band fluorine observation smartprobe. For DOSY experiments, a 10 A z -axis gradient amplifier was employed, with maximum gradient strength of 0.5 T/m. ^1H DOSY was performed using the standard pulse programs (dstebpgp3s), employing a double stimulated echo sequence, bipolar gradient pulses for diffusion, and three spoil gradients. Diffusion time was 100 ms, and the rectangular gradient pulse duration was 1300 μs . Gradient recovery delays were 200 μs . Individual rows of the quasi-2-D diffusion databases were phased and baseline corrected. Actual diffusion coefficients used for D-FW analysis were obtained using the T1/T2 analysis module in commercially available software.

Materials and Methods. Pentane, pinacolone, and diisopropylamine (DIPA) were dried by stirring with calcium hydride (CaH_2) under Ar atmosphere overnight then distillation. Toluene was gained from dry solvent system. Unless otherwise stated, purchased chemicals were used as received. All reactions under anhydrous conditions were conducted using flame- or oven-dried glassware and standard syringe techniques under an atmosphere of argon.

General Procedures for the Crystallization of H_2 . *Method 1.* To a 1.1 M DIPA (5.5 mmol) solution in 5.0 mL pentane at 0 °C under Ar atmosphere was slowly added 2.1 mL 2.5 M *n*-BuLi (5.25 mmol). The reaction mixture was allowed to stir at 0 °C for 10 min. 0.5 g of pinacolone (5 mmol) was then added dropwise, and the mixture was allowed to stir at 0 °C for 15 min. Finally, HMPA 0.18 g (1.0 mmol, 0.15–0.2 equiv) was added, and the solution was kept stirring for another 15 min at room temperature. The clear solution was then stored in a -20 °C freezer, and XRD quality crystals were collected after several days.

Method 2. To a 1.1 M DIPA (5.5 mmol) solution in 5.0 mL of toluene at 0 °C under Ar atmosphere was slowly added 2.1 mL 2.5 M *n*-BuLi (5.25 mmol). The reaction mixture was allowed to stir at 0 °C for 10 min. 0.5 g of pinacolone (5 mmol) was then added dropwise, and the mixture was allowed to stir at 0 °C for 15 min. The clear solution was then stored in a -20 °C freezer, and XRD quality crystals were collected after several days.

Method 3. To a 1.1 M DIPA (5.5 mmol) solution in 5.0 mL of pentane at 0 °C under Ar atmosphere was slowly added 2.1 mL 2.5 M *n*-BuLi (5.25 mmol). The reaction mixture was allowed to stir at 0 °C for 10 min. 0.5 g of pinacolone (5 mmol) was then added dropwise, and the mixture was allowed to stir at 0 °C for 15 min. The clear solution was then stored in a -20 °C freezer, and XRD quality crystals were collected after overnight. Mother liquor was removed via syringe, and dried pentane was added dropwise at 0 °C to fully redissolve the

crystals. Then the clear solution was put back in a -20 °C freezer, and XRD quality crystals were collected after several days.

ASSOCIATED CONTENT

Supporting Information

The Supporting Information is available free of charge on the ACS Publications website at DOI: 10.1021/jacs.6b08177.

NMR data (PDF)

Crystallographic data (CIF)

AUTHOR INFORMATION

Corresponding Author

*pgw@brown.edu

Present Addresses

[†]Velico Medical Inc., 100 Cummings Center, Suite 436H, Beverly, MA 01915, United States.

[‡]Department of Chemistry, The University of Rhode Island, Beapure Hall, 140 Flagg Road, Kingston, RI 02881, United States.

^{||}National Key Lab of Polymer Materials Engineering, Sichuan University, No. 24 South Section 1, Yihuan Road, Chengdu, China, 610065

Notes

The authors declare no competing financial interest.

ACKNOWLEDGMENTS

This work was supported by NSF grant 1058051 to P.G.W.

REFERENCES

- (1) (a) Su, C.; Hopson, R.; Williard, P. G. *J. Org. Chem.* **2013**, *78*, 11733–11746. (b) Reich, H. J.; Sikorski, W. H.; Sanders, A. W.; Jones, A. C.; Plessel, K. N. *J. Org. Chem.* **2009**, *74*, 719–729. (c) Rutherford, J. L.; Hoffmann, D.; Collum, D. B. *J. Am. Chem. Soc.* **2002**, *124*, 264–271. (d) Sun, X.; Winemiller, M. D.; Xiang, B.; Collum, D. B. *J. Am. Chem. Soc.* **2001**, *123*, 8039–8046. (e) Remenar, J. F.; Collum, D. B. *J. Am. Chem. Soc.* **1998**, *120*, 4081–4086. (f) Reich, H. J.; Holladay, J. E.; Mason, J. D.; Sikorski, W. H. *J. Am. Chem. Soc.* **1995**, *117*, 12137–12150. (g) Seebach, D. *Angew. Chem.* **1988**, *100*, 1685–1715. (h) Seebach, D.; Amstutz, R.; Dunitz, J. D. *Helv. Chim. Acta* **1981**, *64*, 2622–2626.
- (2) Poepler, A.-C.; Granitzka, M.; Herbst-Irmer, R.; Chen, Y.-S.; Iversen, B. B.; John, M.; Mata, R. A.; Stalke, D. *Angew. Chem., Int. Ed.* **2014**, *53* (48), 13282–13287.
- (3) (a) Nichols, M. A.; Leposa, C. M.; Hunter, A. D.; Zeller, M. J. *Chem. Crystallogr.* **2007**, *37*, 825–829. (b) Williard, P. G.; Carpenter, G. B. *J. Am. Chem. Soc.* **1985**, *107*, 3345–3346.
- (4) (a) Guang, J.; Liu, Q.; Hopson, R.; Williard, P. G. *J. Am. Chem. Soc.* **2015**, *137*, 7347–7356. (b) Pospisil, P. J.; Wilson, S. R.; Jacobsen, E. N. *J. Am. Chem. Soc.* **1992**, *114*, 7585–7587. (c) Amstutz, R.; Schweizer, W. B.; Seebach, D.; Dunitz, J. D. *Helv. Chim. Acta* **1981**, *64*, 2617–2621.
- (5) (a) Kolonko, K. J.; Guzei, I.; Reich, H. J. *J. Org. Chem.* **2010**, *75*, 6163–6172. (b) Kolonko, K. J.; Biddle, M. M.; Guzei, I.; Reich, H. J. *J. Am. Chem. Soc.* **2009**, *131*, 11525–11534.
- (6) (a) Armstrong, D. R.; Drummond, A. M.; Balloch, L.; Graham, D. V.; Hevia, E.; Kennedy, A. R. *Organometallics* **2008**, *27*, 5860–5866. (b) Laube, T.; Dunitz, J. D.; Seebach, D. *Helv. Chim. Acta* **1985**, *68*, 1373–1393.
- (7) Kolonko, K. J.; Biddle, M. M.; Guzei, I.; Reich, H. J. *J. Am. Chem. Soc.* **2009**, *131*, 11525–11534.
- (8) Williard, P. G.; Hintze, M. J. *J. Am. Chem. Soc.* **1990**, *112*, 8602–8604.
- (9) Amstutz, R.; Dunitz, J. D.; Laube, T.; Schweizer, W. B.; Seebach, D. *Chem. Ber.* **1986**, *119*, 434–443.

- (10) (a) Graser, M.; Kopacka, H.; Wurst, K.; Muller, T.; Bildstein, B. *Inorg. Chim. Acta* **2013**, *401*, 38–40. (b) Apeloig, Y.; Zharov, L.; Bravov-Zhivotovskii, D.; Ovchinnikov, Y.; Struchkov, Y. J. *J. Organomet. Chem.* **1995**, *499*, 73–76. (c) Williard, P. G.; Hintze, M. J. *J. Am. Chem. Soc.* **1987**, *109*, 5539–5541. (d) Jastrzebski, J. T. B. H.; Van Koten, G.; Christophersen, M. J. N.; Stam, C. H. *J. Organomet. Chem.* **1985**, *292*, 319–324.
- (11) (a) Henderson, K. W.; Dorigo, A. E.; Williard, P. G.; Bernstein, P. R. *Angew. Chem., Int. Ed. Engl.* **1996**, *35*, 1322–1324. (b) Henderson, K. W.; Dorigo, A. E.; Liu, Q.-Y.; Williard, P. G.; Schleyer, P. v. R.; Bernstein, P. R. *J. Am. Chem. Soc.* **1996**, *118*, 1339–1347.
- (12) (a) Armstrong, D. R.; Drummond, A. M.; Balloch, L.; Graham, D. V.; Hevia, E.; Kennedy, A. R. *Organometallics* **2008**, *27*, 5860–5866. (b) Hsueh, M.-L.; Ko, B.-T.; Athar, T.; Lin, C.-C.; Wu, T.-M.; Hsu, S.-F. *Organometallics* **2006**, *25*, 4144. (c) Henderson, K. W.; Williard, P. G.; Bernstein, P. R. *Angew. Chem., Int. Ed. Engl.* **1995**, *34*, 1117–1119.
- (13) Collum, D. B. *Acc. Chem. Res.* **1992**, *25*, 448–454.
- (14) (a) Arnett, E. M.; Moe, K. D. *J. Am. Chem. Soc.* **1991**, *113*, 7288–7293. (b) Arnett, E. M.; Fisher, F. J.; Nichols, M. A.; Ribeiro, A. A. *J. Am. Chem. Soc.* **1990**, *112*, 801–808. (c) Seebach, D.; Bauer, W. *Helv. Chim. Acta* **1984**, *67*, 1972–1988.
- (15) (a) Streitwieser, A. *J. Mol. Model.* **2006**, *12*, 673–680. (b) Kim, Y.-J.; Streitwieser, A. *Org. Lett.* **2002**, *4*, 573–575. (c) Streitwieser, A.; Kim, Y.-J.; Wang, D. Z.-R. *Org. Lett.* **2001**, *3*, 2599–2601. (d) Wang, D. Z.; Kim, Y.-J.; Streitwieser, A. *J. Am. Chem. Soc.* **2000**, *122*, 10754–10760. (e) Streitwieser, A.; Wang, D. Z. *J. Am. Chem. Soc.* **1999**, *121*, 6213–6219. (f) Leung, S. S.-W.; Streitwieser, A. *J. Org. Chem.* **1999**, *64*, 3390–3391. (g) Streitwieser, A.; Leung, S. S.-W.; Kim, Y.-J. *Org. Lett.* **1999**, *1*, 145–147. (h) Abbotto, A.; Leung, S. S.-W.; Streitwieser, A.; Kilway, K. V. *J. Am. Chem. Soc.* **1998**, *120*, 10807–10813. (i) Leung, S. S.-W.; Streitwieser, A. *J. Am. Chem. Soc.* **1998**, *120*, 10557–10558. (j) Abu-Hasanayn, F.; Streitwieser, A. *J. Org. Chem.* **1998**, *63*, 2954–2960. (k) Abu-Hasanayn, F.; Streitwieser, A. *J. Am. Chem. Soc.* **1996**, *118*, 8136–8137. (l) Gareyev, R.; Ciula, J. C.; Streitwieser, A. *J. Org. Chem.* **1996**, *61*, 4589–4593. (m) Abu-Hasanayn, F.; Stratakis, M.; Streitwieser, A. *J. Org. Chem.* **1995**, *60*, 4688–4689. (n) Dixon, R. E.; Williams, P. G.; Saljoughian, M.; Long, M. A.; Streitwieser, A. *Magn. Reson. Chem.* **1991**, *29*, 509–512.
- (16) Jackman, L. M.; Szeverenyi, N. M. *J. Am. Chem. Soc.* **1977**, *99*, 4954–4962.
- (17) (a) Reich, H. J. *J. Org. Chem.* **2012**, *77*, 5471–5491. (b) Kolonko, K. J.; Guzei, L. A.; Reich, H. J. *J. Org. Chem.* **2010**, *75*, 6163–6172. (c) Kolonko, K. J.; Biddle, M. M.; Guzei, L. A.; Reich, H. J. *J. Am. Chem. Soc.* **2009**, *131*, 11525–11534.
- (18) (a) Jin, K. J.; Collum, D. B. *J. Am. Chem. Soc.* **2015**, *137*, 14446–14455. (b) Tomasevich, L. L.; Collum, D. B. *J. Am. Chem. Soc.* **2014**, *136*, 9710–9718. (c) Renny, J. S.; Tomasevich, L. L.; Tallmadge, E. H.; Collum, D. B. *Angew. Chem., Int. Ed.* **2013**, *52*, 11998–12013. (d) Liou, L. R.; McNeil, A. J.; Ramirez, A.; Toombes, G. E. S.; Gruver, J. M.; Collum, D. B. *J. Am. Chem. Soc.* **2008**, *130*, 4859–4868. (e) Liou, L. R.; McNeil, A. J.; Toombes, G. E. S.; Collum, D. B. *J. Am. Chem. Soc.* **2008**, *130*, 17334–17341. (f) Gruver, J. M.; Liou, L. R.; McNeil, A. J.; Ramirez, A.; Collum, D. B. *J. Org. Chem.* **2008**, *73*, 7743–7747.
- (19) Li, D.; Keresztes, I.; Hopson, R.; Williard, P. G. *Acc. Chem. Res.* **2009**, *42*, 270–280.
- (20) (a) Bachmann, S.; Neufeld, R.; Dzemski, M.; Stalke, D. *Chem. - Eur. J.* **2016**, *22* (25), 8462–8465. (b) Neufeld, R.; Stalke, D. *Chem. Sci.* **2015**, *6*, 3354–3364. (c) Evans, R.; Deng, Z.; Rogerson, A. K.; McLachlan, A. S.; Richards, J. J.; Nilsson, M.; Morris, G. A. *Angew. Chem., Int. Ed.* **2013**, *52*, 3199–3202.
- (21) Cruz-Cabeza, A. J.; Bernstein, J. *Chem. Rev.* **2014**, *114*, 2170–2191.
- (22) Williard, P. G.; Carpenter, G. B. *J. Am. Chem. Soc.* **1986**, *108*, 462–468.
- (23) (a) Bucar, D.-K.; Lancaster, R. W.; Bernstein, J. *Angew. Chem., Int. Ed.* **2015**, *54*, 6972–6993. (b) Dunitz, J. D.; Bernstein, J. *Acc. Chem. Res.* **1995**, *28*, 193–200.
- (24) Ostwald, W. Z. *Phys. Chem.* **1897**, *22*, 289–330.
- (25) (a) Threlfall, T. *Org. Process Res. Dev.* **2003**, *7*, 1017–1027. (b) Mullin, J. W. *Crystallization*, 3rd ed.; Butterworth-Heinemann: Oxford, 1993.
- (26) Hevia, E.; Kennedy, A. R.; Mulvey, R. E.; Ramsay, D. L.; Robertson, S. D. *Chem. - Eur. J.* **2013**, *19* (42), 14069–14075.
- (27) Harrison-Marchand, A.; Mongin, F. *Chem. Rev.* **2013**, *113*, 7470–7562.
- (28) Williard, P. G.; Liu, Q. Y. *J. Am. Chem. Soc.* **1993**, *115*, 3380–3381.
- (29) (a) Berke, H. *Main Group Met. Chem.* **1991**, *14*, 137–152. (b) Williard, P. G.; Salvino, J. M. *Tetrahedron Lett.* **1985**, *26*, 3931–3934.
- (30) (a) Tallmadge, E. H.; Jermaks, J.; Collum, D. B. *J. Am. Chem. Soc.* **2016**, *138*, 345–355. (b) Larranaga, O.; Cozar, A.; Bickelhaupt, F. M.; Zangi, R.; Cossio, F. P. *Chem. - Eur. J.* **2013**, *19*, 13761–13773. (c) Collum, D. B.; McNeil, A. J.; Ramirez, A. *Angew. Chem., Int. Ed.* **2007**, *46*, 3002–3017. (d) Jones, A. C.; Sanders, A. W.; Bevan, M. J.; Reich, H. J. *J. Am. Chem. Soc.* **2007**, *129*, 3492–3493.
- (31) Kolonko, K.; Wherritt, D. J.; Reich, H. J. *J. Am. Chem. Soc.* **2011**, *133*, 16774–16777.
- (32) Ma, J. C.; Dougherty, D. A. *Chem. Rev.* **1997**, *97*, 1303–1324.
- (33) Moakes, G.; Daemen, L. L.; Gelbaum, L. T.; Leisen, J.; Marecek, V.; Janata, J. *J. Phys. Chem. B* **2007**, *111* (25), 7312–7317.
- (34) Gilchrist, J. H.; Collum, D. B. *J. Am. Chem. Soc.* **1992**, *114*, 794–795.
- (35) Henderson, K. W.; Dorigo, A. E.; MacEwan, G. J.; Williard, P. G. *Tetrahedron* **2011**, *67*, 10291–10295.